Computational study of neutral and cationic catacondensed polycyclic aromatic hydrocarbons

ARTICLE *in* CHEMICAL PHYSICS · JUNE 2005

Impact Factor: 1.65 · DOI: 10.1016/j.chemphys.2005.01.007

2 AUTHORS:

Amit Pathak
Tezpur University
28 PUBLICATIONS **134** CITATIONS
SEE PROFILE

Shantanu Rastogi
Maimonides Medical Center
56 PUBLICATIONS **520** CITATIONS
SEE PROFILE

Amit Pathak, Sha

ment of Physics, D.D.U. Gorakhpur University, Gorakhp

Received 31 July 2004; accepted 7 January 2005
Available online 26 January 2005

Abstract

Theoretical calculations have been done for neutral and cationic catacondensed polycyclic aromatic hydrocarbons (PAH) using density functional theory approach. Optimized geometries and charge distributions have been calculated and the change in structure and charge distribution upon ionization of PAHs is studied and discussed. The calculated infrared vibrational modes show systematic variations with size in the linear polyacenes while no regular variation is apparent in non-linear catacondensed PAHs. The prominent features in the spectra of neutral PAHs are due to C–H stretch and C–H wag motions. In the spectra of PAH cations C–C stretch and C–H in plane modes are the most intense. The changes in charge distributions of cations causing these intensity changes have been identified. The C–H stretch intensity depends on the partial charge on peripheral Hydrogen atoms and reduces in cations as Hydrogen atoms become more positive. The prospect of catacondensed PAHs is discussed in the context of Astrophysical Unidentified Infrared bands.

Keywords: PAH; Interstellar molecules; DFT; Charge distribution; IR spectra; Aromatic infrared bands

1. Introduction

The mid infrared spectra of many Astronomical sources like HII regions, Planetary Nebulae, Reflection Nebulae, Post AGB stars, star forming regions, Interstellar medium (ISM) of our galaxy and even of outer galaxies show distinct emission features at 3.3, 6.2, 7.7, 8.6 and 11.2 μm (3030, 1610, 1300, 1160, 890 cm^{-1}) [1–6]. These ubiquitous bands, earlier known as the unidentified infrared (UIR) bands, arise from vibrations within molecules having Aromatic moieties. Due to their Aromatic origin these bands are now also known as aromatic infrared bands (AIBs). Polycyclic aromatic hydrocarbon (PAH) molecules are proposed as the most viable carriers of these bands [7–10], though identification of a specific PAH has not yet been possible. PAHs seem to be partially responsible for the UV extinction bump at 217 nm [11] and are also considered to be strong candidates for the carriers of diffuse interstellar bands (DIBs) [12–15], which are emission features superimposed on the interstellar extinction curve.

The PAH molecules consist of several benzenoid rings forming a planar structure. They have a highly stable configuration due to the entire de-localization of π electrons over the whole molecule. The large cross-section area of PAHs makes them efficient absorber of the background radiation. Depending on the strength of the background UV field the molecules may dissociate, get ionized or dehydrogenated. The molecule may also experience structural reformation to a more compact and stable configuration. A PAH molecule may get vibrationally heated upto a temperature of 1000 K by the absorption of a single UV photon. It then undergoes 'internal vibrational redistribution' to distribute the

* Corresponding author. Tel.: +915512204517; fax: +915512330767.
E-mail address: shantanu_r@hotmail.com (S. Rastogi).

0301-0104/$ - see front matter © 2005 Elsevier B.V. All rights reserved.
doi:10.1016/j.chemphys.2005.01.007

absorbed energy over different vibrational modes. The molecule de-excites through IR Fluorescence [9,10]. Larger PAH molecules are easily ionized so the overall IR spectrum should result from a mixture of neutral and ionized PAHs.

Several laboratory spectroscopic studies in Matrix Isolation [16–29] and in Gas phase [30–34] have been done on small PAHs in their neutral and ionized forms. Theoretical ab initio and normal mode calculations [35–40] have also been reported to complement the experimental results. These reports reinforce the interstellar PAH hypothesis and show that PAH cations have a better intensity correlation with AIBs than neutrals. The band positions for ionized PAHs differ little from neutrals but there is remarkable difference in the intensity patterns.

In order to understand the vibrational spectra of PAHs and its variation with the change in size and ionization state of the molecules, we report a detailed theoretical study of catacondensed PAHs. The effect of ionization on the charge distribution and its relation to the significant changes occurring in the IR spectra of these PAHs is discussed. Astrophysical implications have been presented to obtain better correlation with the AIBs.

Density functional theory (DFT) is employed in this theoretical study of catacondensed PAHs using the GAMESS [41] ab initio program. First optimized geometries of all the molecules were obtained using B3LYP functionals in conjunction with 4-31G basis expansion. The IR frequencies of neutrals are calculated using restricted Hartree–Fock (RHF) method. Calculations for cations are done using unrestricted Hartree–Fock (UHF) instead of the restricted open-shell Hartree–Fock (ROHF) wave functions. For open shell systems orbital energies from ROHF wave function are not uniquely defined whereas the UHF treatment leads to well defined orbital energies since there are no restrictions on the form of spatial orbitals [42]. The UHF function was therefore chosen for PAH cations even at the cost of extra computational time. The computed IR spectra of each PAH is plotted considering Gaussian peaks with full-width at half-maximum to be 30 cm^{-1}. The peak width depends on the internal vibrational redistribution time of the molecule and 30 cm^{-1} is the typical width for PAHs emitting in conditions similar to those of the ISM [10].

2. Results

Large intensity variations are present in the spectra of the ionized species in comparison to the neutrals. These

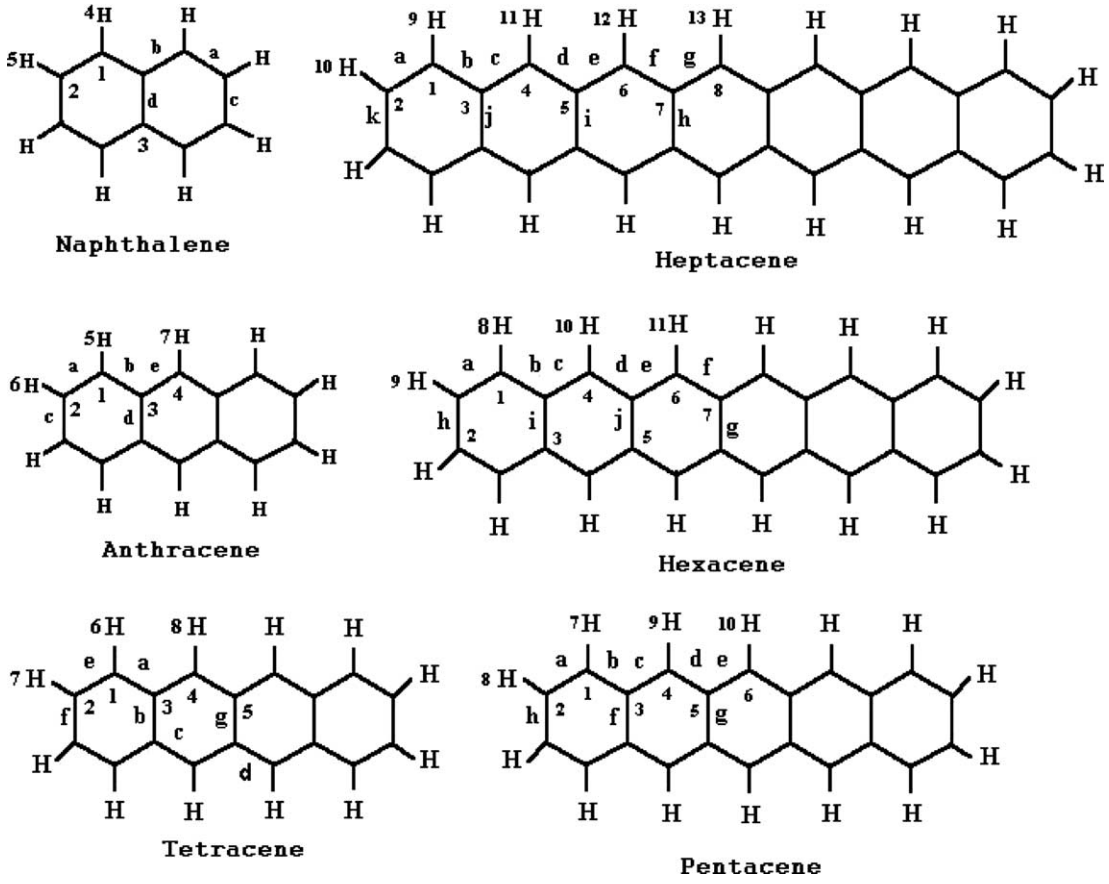

Fig. 1. Linear PAHs; only symmetry unique atoms and bonds are labeled.

variations may be related to the change in charge distribution and subsequent dipole moment variations. In this context the charge distribution of various neutral and ionized catacondensed PAH molecules have been studied. The point group symmetry of the molecules is retained in the ionized species. The bond lengths of both neutral and ionized PAHs is compared to get a picture of the effect of ionization on the structure of molecules. For studying the systematic variations with size linear catacondensed PAHs, Fig. 1, are considered from Naphthalene (2 rings) to Heptacene (7 rings). Phenanthrene, Chrysene and 3,4-Benzophenanthrene are the non-linear catacondensed PAHs studied, Fig. 2.

2.1. Charge distribution

With the removal of one electron from the π system of PAH, nearly all the atoms of the molecule acquire a more positive charge. The change in the charges of the atoms depends on the structure of the molecule and the atom's position in a particular molecule. The ionization of PAHs does not affect its symmetry, the structure suffers minor changes mainly in the bond length while negligible changes are there in the bond angles as also reported by DeFrees et al. [37] for Naphthalene, Anthracene and Pyrene. Upon ionization the linear PAHs show similar changes in their bond lengths and charge distributions while the non-linear PAHs are very much different from the linear ones and from each other as well. The charge distributions and bond lengths of the studied PAHs is given in Table 1. Mulliken population generated by the geometry optimization of each PAH is taken as the charge on atoms. The Carbon atoms on the edges of the rings having a bond with Hydrogen atoms have been taken as outer atoms while all other Carbon atoms are inner.

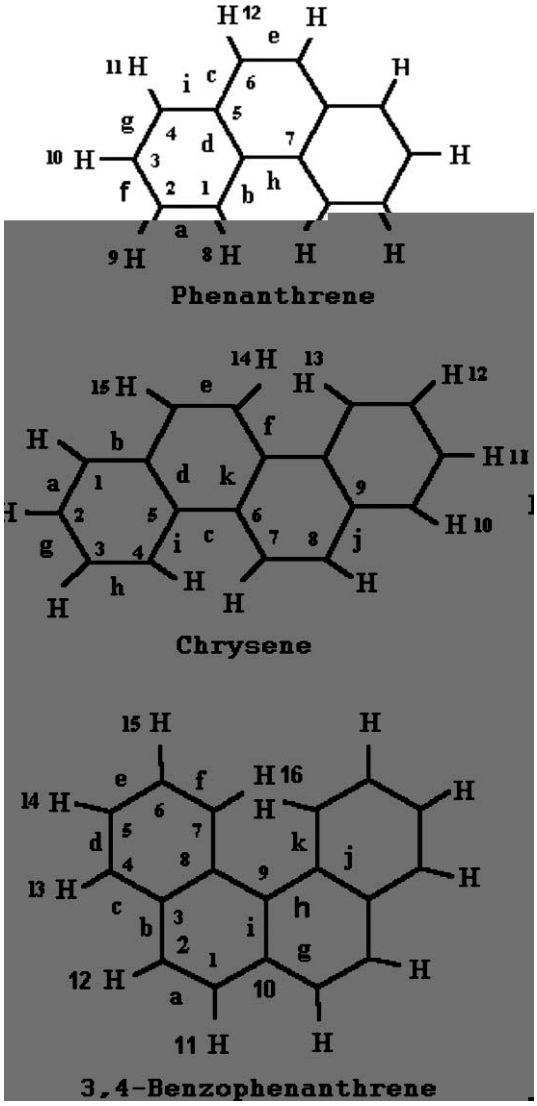

Fig. 2. Non-linear PAHs; only symmetry unique atoms and bonds are labeled.

2.1.1. Linear PAHs

Electronegative Carbon carries a partial negative charge, while Hydrogen has a partial positive charge. But in neutral PAHs, all the inner Carbon atoms have partial positive charge while the outer ones are negative. Upon ionization all the Hydrogen atoms have acquired a more positive charge. The charges of the Carbon atoms located on the outer edges of the rings have changed to a less negative value while the changes in the charges of the inner Carbon atoms is insignificant.

Linear polyacenes when ionized show major bond length changes (elongation or contraction) in the outer bonds while the inner bonds remain unchanged. PAH molecules having even number of rings have no bond length changes in the central structure of the molecule while PAHs with odd number of rings have no bond length changes in the central ring. The C–H bond lengths do not change upon ionization. Both the change in charge distribution and bond lengths occurs mainly in the outer structure for all polyacenes.

2.1.2. Non-linear PAHs

The changes occurring in the charges and bond lengths upon ionization of non-linear catacondensed PAHs are very different from the linear ones except for the change in charges of the Hydrogen atoms and C–H bond lengths which is similar to those in linear PAHs.

Upon ionization, Phenanthrene shows changes in charges of outer Carbon atoms and outer bond lengths with a few exceptions. Charge on outer Carbons C1 and C3 change a little while C7 an inner atom, shows significant positive increase in charge. The length of outer bonds *f* and *g* do not change while there is significant change in lengths of other bonds.

In Chrysene, upon ionization the outer Carbons C2, C4 and C7 show small changes in their charges while,

Table 1
Bond length and charge distribution of studied PAHs

Bond lengths			Charge distribution		
Bonds[a]	Neutral	Cation	Atoms[a]	Neutral	Cation
Naphthalene					
a	1.380	1.406	C1	−0.143	−0.091
b	1.420	1.414	C2	−0.128	−0.095
c	1.416	1.391	C3	0.038	0.037
d	1.440	1.436	H4	0.127	0.208
			H5	0.126	0.210
Anthracene					
a	1.369	1.391	C1	−0.138	−0.110
b	1.430	1.414	C2	−0.131	−0.103
c	1.425	1.404	C3	0.046	0.042
d	1.448	1.444	C4	−0.189	−0.118
e	1.399	1.409	H5	0.128	0.189
			H6	0.127	0.194
			H7	0.127	0.194
Tetracene					
a	1.434	1.418	C1	−0.136	−0.119
b	1.455	1.448	C2	−0.132	−0.108
c	1.391	1.406	C3	0.046	0.045
d	1.409	1.405	C4	−0.189	−0.141
e	1.366	1.382	C5	0.056	0.048
f	1.429	1.413	H6	0.128	0.177
g	1.455	1.453	H7	0.127	0.184
			H8	0.128	0.183
Pentacene					
a	1.365	1.376	C1	−0.135	−0.123
b	1.436	1.422	C2	−0.132	−0.112
c	1.388	1.402	C3	0.046	0.047
d	1.414	1.404	C4	−0.189	−0.148
e	1.401	1.405	C5	0.057	0.049
f	1.458	1.451	H6	−0.190	0.140
g	1.460	1.457	H7	0.129	0.169
h	1.431	1.418	H8	0.127	0.176
			H9	0.128	0.174
			H10	0.128	0.177
Hexacene					
a	1.364	1.373	C1	−0.134	−0.125
b	1.436	1.426	C2	−0.132	−0.115
c	1.386	1.399	C3	0.046	0.048
d	1.416	1.405	C4	−0.189	−0.157
e	1.397	1.405	C5	0.057	0.049
f	1.406	1.403	C6	−0.189	−0.148
g	1.463	1.462	C7	0.057	0.049
h	1.432	1.422	H8	0.129	0.163
i	1.460	1.453	H9	0.128	0.169
j	1.462	1.459	H10	0.129	0.167
			H11	0.129	0.171
Heptacene					
a	1.364	1.371	C1	−0.134	−0.127
b	1.437	1.428	C2	−0.132	−0.117
c	1.385	1.396	C3	0.046	0.049
d	1.417	1.407	C4	−0.188	−0.163
e	1.395	1.404	C5	0.057	0.054
f	1.408	1.402	C6	−0.189	−0.155
g	1.402	1.404	C7	0.057	0.051
h	1.465	1.464	C8	−0.189	−0.151
i	1.463	1.460	H9	0.129	0.158
j	1.461	1.455	H10	0.128	0.165
k	1.433	1.424	H11	0.129	0.162
			H12	0.129	0.166
			H13	0.129	0.168

Table 1 (*continued*)

Bond lengths			Charge distribution		
Bonds[a]	Neutral	Cation	Atoms[a]	Neutral	Cation
Phenanthrene					
a	1.383	1.403	C1	−0.139	−0.127
b	1.414	1.397	C2	−0.129	−0.089
c	1.433	1.404	C3	−0.122	−0.109
d	1.430	1.441	C4	−0.152	−0.102
e	1.358	1.399	C5	0.033	0.031
f	1.407	1.403	C6	−0.142	−0.109
g	1.380	1.380	C7	0.012	0.046
h	1.458	1.466	H8	0.131	0.181
i	1.414	1.428	H9	0.126	0.195
			H10	0.127	0.192
			H11	0.127	0.190
			H12	0.128	0.202
Chrysene					
a	1.379	1.388	C1	−0.148	−0.115
b	1.417	1.416	C2	−0.123	−0.106
c	1.452	1.459	C3	−0.129	−0.103
d	1.427	1.428	C4	−0.135	−0.121
e	1.364	1.387	C5	0.000	−0.024
f	1.431	1.406	C6	0.001	0.035
g	1.410	1.399	C7	−0.129	−0.126
h	1.381	1.397	C8	−0.146	−0.104
i	1.417	1.405	C9	0.038	0.029
j	1.427	1.418	H10	0.128	0.179
k	1.417	1.447	H11	0.127	0.184
			H12	0.126	0.183
			H13	0.131	0.172
			H14	0.132	0.179
			H15	0.128	0.189
3,4-Benzophenanthrene					
a	1.353	1.360	C1	−0.147	−0.138
b	1.423	1.426	C2	−0.142	−0.105
c	1.416	1.405	C3	0.022	0.022
d	1.375	1.393	C4	−0.145	−0.124
e	1.404	1.391	C5	−0.126	−0.098
f	1.383	1.395	C6	−0.127	−0.109
g	1.427	1.414	C7	−0.154	−0.127
h	1.478	1.470	C8	0.034	0.039
i	1.428	1.471	C9	0.034	0.044
j	1.443	1.443	C10	0.006	0.039
k	1.423	1.421	H11	0.129	0.183
			H12	0.130	0.188
			H13	0.128	0.183
			H14	0.128	0.189
			H15	0.126	0.182
			H16	0.138	0.173

[a] For bond labeling and atom numbering refer to Figs. 1 and 2.

C5 and C6 being inner Carbons show significant effect of ionization. The charge on C5 changes to a more negative character and the charge on C6 changes to a higher positive value. Upon ionization, though the outer bonds show significant change in lengths except for bonds *a* and *g*, the maximum change in length is for the inner central bond *k*.

In 3,4-Benzophenanthrene, neutral and cation, the distance between bay region Hydrogen atoms (H16) is about 1.55 Å, which is smaller than the distance between two non-bonded neighbouring H atoms in organic molecules. This causes steric hindrance between these H atoms resulting in a slight asymmetric structure. C1 an outer Carbon shows small change in its charge while C10 an inner Carbon shows a larger change. Bond *a* an outer bond shows very little change on ionization whereas bond *i*, the inner central bond shows the maximum change in length.

In terms of charge distribution and bond length changes upon ionization the non-linear PAHs behave differently from linear PAHs. While only the outer atoms and bonds get affected in case of polyacenes, a

few inner atoms and bonds also show significant ionization effect in non-linear PAHs. As a result of ionization, the maximum change in bond length is for the central bond of the molecule in case of non-linear PAHs while the central structure of linear PAHs remain largely unaffected.

2.2. Vibrational frequencies and intensities

The vibrational frequencies and intensities have been calculated using the 4-31G basis expansion and B3LYP functionals. An excellent match with experimental frequencies have been obtained by the use of a single scale factor of 0.956. For large aromatic molecules, only one scaling factor is required with 4-31G basis [35,43], therefore, the use of any other higher basis set is deferred. The comparisons of our result with the reported experimental data shows very limited discrepancies with the average error in band position match being less than 1%. The maximum error in the band position match with the experimental data is of 25 cm^{-1} (for 1333.3 cm^{-1} mode in Tetracene cation). The average error is even lower in case of the neutral species. The intensities are scaled relative to the intensity of the most intense band. These relative intensities also compare well with the experimental values. The only major discrepancy present is that compared to the experimental intensity, the C–H stretch intensity is overestimated. Using larger basis sets may reduce the magnitude of this anomaly. The calculated vibrational frequencies for Naphthalene using larger basis sets, i.e., 6-31G and 6-311G** does show smaller values for C–H stretch intensity in comparison to the 4-31G basis set. But the use of such higher basis complicates the scaling procedure. Yoshida et al. [44,45] have adopted a wavenumber linear scaling (WLS) method for scaling the frequencies of small molecules obtained using 6-311G** basis set. The WLS method is based on the linear relationship between the scale factor and the vibrational wavenumbers and requires adjustment of two parameters. Our calculations

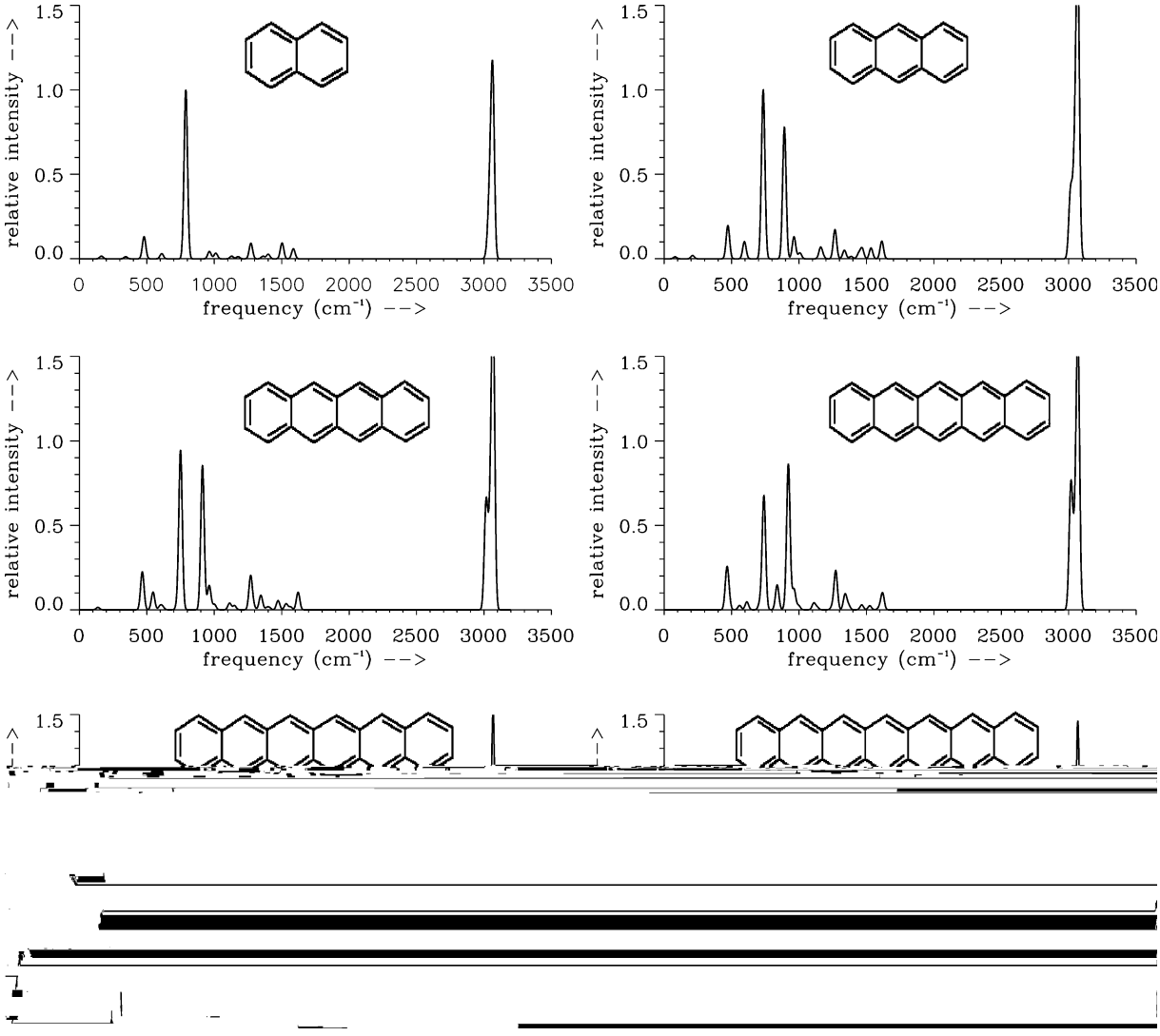

Fig. 3. Computed spectra of linear neutral PAHs.

are for larger molecules and a good match is obtained with a single parameter frequency independent scale factor.

The calculated frequencies and the corresponding intensities are in good agreement with reported experimental and theoretical data. The comparison tables for Naphthalene, Anthracene, Tetracene, Pentacene, Phenantheren and Chrysene are not being given, to save space. These may be obtained from the authors upon request. Charge distribution significantly affects the infrared intensities. The vibrational modes having a very small dipole change in neutral PAHs show large dipole variations upon ionization. The spectra of the neutral PAH molecules mainly consists of C–H out of plane bend mode and C–H stretch modes. On the other hand the spectra of the cations is richer in the C–C stretch and C–H in plane bend modes.

2.2.1. Neutral PAHs

Computed spectra of all linear PAHs studied is shown in Fig. 3. For all the molecules maximum intensities are confined mainly to the C–H stretch vibrations and C–H out of plane vibrations. No intense feature is present in the 1000–1600 cm^{-1} range. Naphthalene having just two rings shows prominent features at 788.8 cm^{-1}, due to wag motion of the quarto Hydrogens, and 3062.6 cm^{-1}, corresponding to the C–H stretch motions. The calculated band at 1502.5 cm^{-1} corresponds to the reported experimental [24] feature at 1498.9 cm^{-1} but the theoretical relative intensity is several times higher.

Anthracene has two intense peaks at 734.6 and 891.4 cm^{-1} for the C–H out of plane bend vibrations. The additional peak is due to the presence of extra solo Hydrogen atoms on the central ring. The band at 1613.9 cm^{-1} corresponds to the experimental [24] one at 1610.5 cm^{-1} but does not match in intensity. The relative intensity of the theoretical band is nearly five times the experimental band.

The band positions of other linear PAHs namely Tetracene, Pentacene, Hexacene and Heptacene are similar to that of the Anthracene spectra. The comparisons with the experimental data shows good match with a few exceptions. In Tetracene the band at 1269.6 cm^{-1} is an order of magnitude more intense than the corresponding experimental [24] feature at 1288.5 cm^{-1}. For Pentacene the computed band at 1272.2 cm^{-1} corresponding to the experimental [25] band at 1269.0 cm^{-1} is more than an order of magnitude higher in intensity.

Table 2

Computed result			
Hexacene		Heptacene	
Freq. (cm^{-1})	Rel. Int.	Freq. (cm^{-1})	Rel. Int.
(a) Band positions and relative intensities of neutral Hexacene and Heptacene			
462.6	0.08	459.9	0.09
742.5	0.59	463.1	0.09
866.1	0.14	594.5	0.08
925.5	0.89	740.6	0.50
962.9	0.11	883.2	0.13
1274.6	0.28	927.4	0.95
1346.4	0.08	963.2	0.09
1616.2	0.09	1275.9	0.36
3015.3	0.58	1357.5	0.07
3016.5	0.13	1619.0	0.07
3043.9	0.23	3016.4	0.49
3064.2	0.53	3043.6	0.20
3070.0	1.00	3044.8	0.46
		3069.8	1.00
(b) Band positions and relative intensities of Hexacene and Heptacene cation			
755.8	0.08	753.7	0.06
950.4	0.08	951.1	0.07
1176.5	0.10	1167.9	0.11
1236.9	0.77	1226.5	0.94
1278.8	0.06	1278.2	0.06
1304.1	0.09	1350.5	0.61
1354.9	1.00	1362.4	0.27
1478.7	0.13	1375.5	0.12
1490.2	0.98	1474.7	0.07
3087.4	0.06	1483.2	1.00
		3085.7	0.06

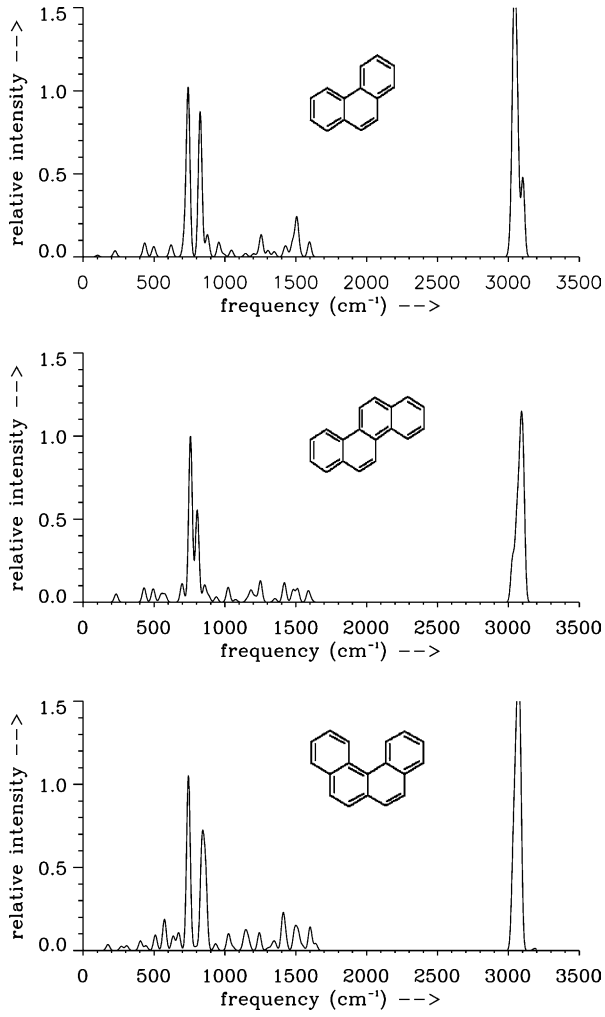

Fig. 4. Computed spectra of non-linear neutral PAHs.

Table 2 gives the theoretically calculated frequencies of Hexacene and Heptacene. No experimental and theoretical results are available for comparison. Their spectra is similar to other linear PAHs except that there is a rise in intensity of the C–H solo wag in comparison to the C–H quarto wag intensity. This characteristic distinguishes them from the smaller members of the polyacene family.

The spectra of linear PAHs shows a general trend in variation of band position and intensity with size. The total integrated intensity of the C–H stretch vibrations is seen to have increased with increasing size of the PAHs. Overall a good intensity correlation exists with the experimental results. The intensity mismatch is mainly in two C–C stretch modes around 1600 and 1265 cm^{-1}. The experimental intensities corresponding to these modes are suppressed in comparison to the theoretical values. The calculated band around 1265 cm^{-1} shifts blue-wards and its absolute intensity increases with size of PAHs.

The computed spectra for non-linear PAHs: Phenanthrene, Chrysene and 3,4-Benzophenanthrene, are shown in Fig. 4. Because of the lower symmetry of these molecules the intensity is distributed over more number of modes leading to a spectra more complex than the spectra of the linear molecules.

For Phenanthrene the most intense peak at 740.7 cm^{-1} is due to quarto out of plane wag and the peak at 840 cm^{-1} is due to duo out of plane wag. C–H stretch modes have significant intensity and consist of a number of moderate peaks. The theoretical bands at 1506.7 and 1596.5 cm^{-1} are assigned to experimental [24] features at 1505.9 and 1597.9 cm^{-1} but their relative intensities do not match. The experimental intensities are lower compared to the theoretical values.

For Chrysene the 756.9 cm^{-1} mode is most intense. The band at 804.7 cm^{-1} arising due to the out of plane motion of duo Hydrogens is lower in intensity in comparison to the corresponding feature in Phenanthrene. The band at 1512.6 cm^{-1} is more intense than its experimental [24] counterpart at 1523.2 cm^{-1}.

Band positions and relative intensities of 3,4-Benzophenanthrene are compared with the gas phase IR data (NIST Chemistry Web Book; http://webbook.nist.gov/chemistry) and with previous theoretical result [35] in Table 3(a). The spectra of this molecule is complex because of the bay region asymmetry, yet a good match with the band positions as well as the relative intensities is obtained. Our calculation predicts the most intense feature at 741.9 cm^{-1} corresponding mainly to quarto Hydrogen wag motion. Two duo Hydrogen wag modes of similar intensity are calculated at 838.5 and 862.3 cm^{-1}. These modes have little contributions of quarto Hydrogens as well. Langhoff [35] reports two quarto modes at 750.4 and 757.7 cm^{-1} and one duo mode at 839.4 cm^{-1}. Our result compares better with the experimental spectra which shows maximum intensity band at 746 cm^{-1} and two modes at 806 cm^{-1} and 886 cm^{-1} with similar intensity.

The intensity comparisons between the calculated and experimental results show good match with very few discrepancies. Theoretical intensities are always higher than experimental values wherever intensity mismatches are present. This suppression of experimental intensity may be due to intra-molecular interactions or matrix effects in the matrix isolated experimental spectra [24,25].

2.2.2. PAH cations

Ionization of PAH molecules brings about dramatic intensity variations and cations show a better intensity correlation with the AIBs [35,46]. The calculated spectra of ionized PAH molecules, Fig. 5, shows increase of intensity in the 1000–1600 cm^{-1} range. The most intense feature being near 1300 cm^{-1} (corresponding to the 7.7 μm band of the AIBs). The intensity of the C–H

Table 3

Computed result		Experimental result[a]		Theoretical result[b]	
Freq. (cm^{-1})	Rel. Int.	Freq. (cm^{-1})	Rel. Int.	Freq. (cm^{-1})	Rel. Int.
(a) Comparison of band positions and relative intensities of neutral 3,4-Benzophenanthrene					
508.9	0.09			508.6	0.12
573.4	0.19			578.9	0.16
634.5	0.09			627.9	0.11
672.8	0.11			673.9	0.13
741.9	1.00	746	1.00	750.4	0.52
752.4	0.07			757.7	0.56
838.5	0.61	806	0.32	839.4	1.00
862.3	0.47	886	0.53	872.5	0.21
934.3	0.04	950	0.07	951.0	0.08
1025.2	0.10	1042	0.06		
1142.1	0.08	1130	0.04		
1242.7	0.11	1242	0.13	1237.3	0.16
1409.4	0.20	1386	0.12	1418.3	0.21
1492.8	0.12	1502	0.15	1494.0	0.17
1517.5	0.09				
1602.7	0.08				
3032.9	0.20				
3035.7	0.22				
3040.6	0.15			3046.1	0.08
3054.6	0.57			3056.5	0.19
3057.6	0.62	3066	0.77	3058.2	0.20
3067.1	0.36			3064.1	0.30
				3066.7	0.98
3077.6	0.63			3075.9	0.95
3084.2	0.58			3077.4	0.42
				3120.5	0.15
3246.0	0.19	3194	0.01		
(b) Comparison of band positions and relative intensities of 3,4-Benzophenanthrene cation					
277.6	0.07	317.2	0.04		
409.5	0.13	406.2	0.04		
476.0	0.05	486.5	0.05		
492.1	0.02	494.1	0.04		
558.4	0.03	563.4	0.04		
621.7	0.05	614.7	0.05		
742.5	0.15	749.7	0.11		
		756.1	0.18		
852.4	0.06	854.8	0.24		
884.1	0.09	896.1	0.07		
1027.9	0.05	1034.3	0.10		
1070.5	0.89				
		1111.3	0.49		
1124.3	0.06	1127.7	0.44		
		1182.2	0.16		
1203.8	1.00	1215.2	0.83		
1206.8	0.05	1216.6	0.16		
1212.6	0.33	1219.7	0.95		
1241.9	0.11	1237.6	0.12		
1244.5	0.09				
1282.3	0.39				
1297.9	0.70	1299.0	1.00		
		1346.1	0.97		
1399.1	0.43	1399.7	0.91		
1416.2	0.05				
1441.5	0.49	1437.8	0.45		
		1523.4	0.66		
1551.9	0.65	1552.3	0.99		
3109.0	0.02	3106.0	0.04		

[a] NIST Chemistry Web Book IR data (http://webbook.nist.gov/chemistry).
[b] Ref. [35].

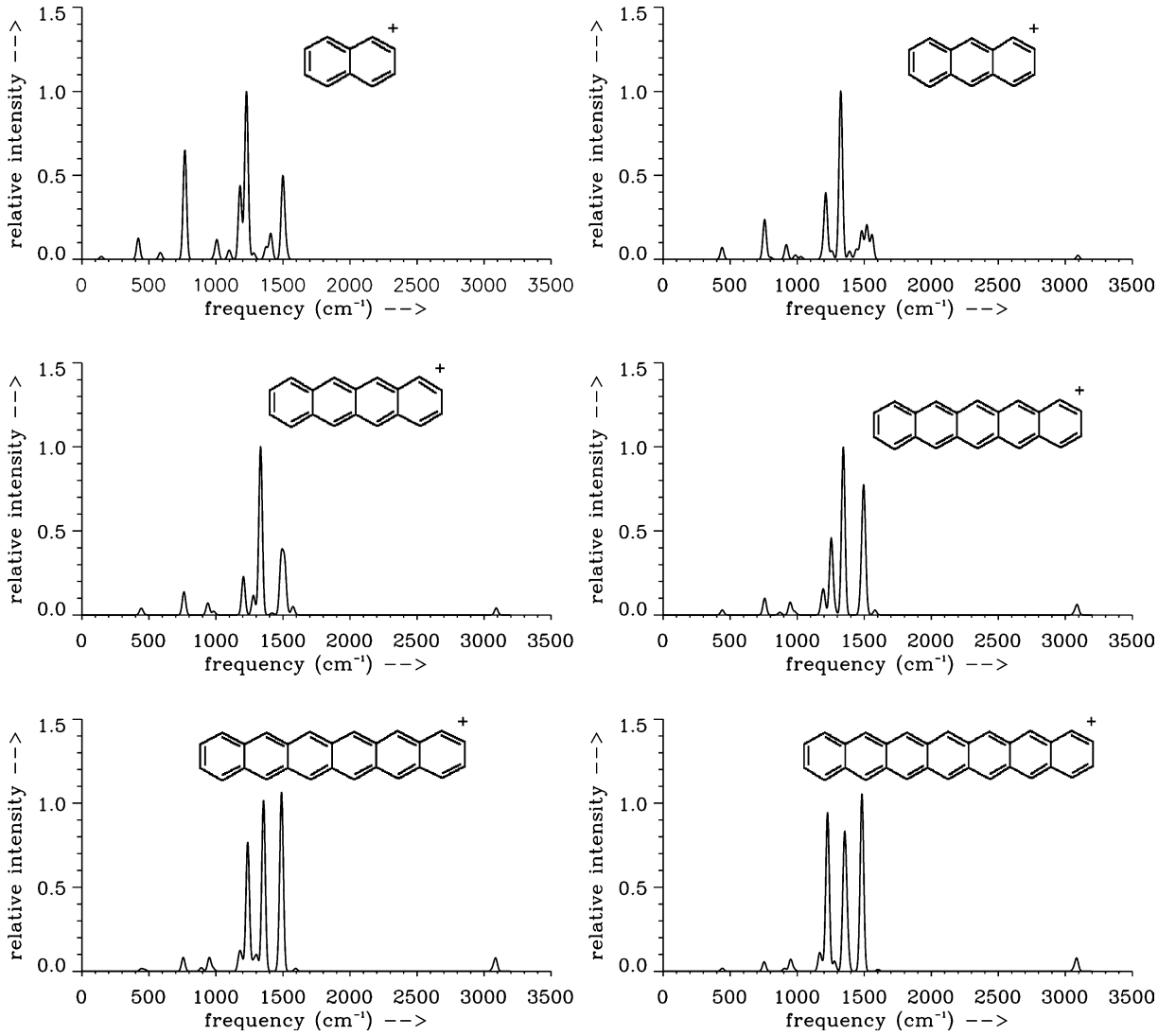

Fig. 5. Computed spectra of linear PAH cations.

stretch modes have reduced drastically while there is very little effect on the absolute intensity of the C–H out of plane bend modes.

A number of intense and moderate features for Naphthalene cation are present in the 1100–1500 cm^{-1} range with the maximum intensity mode at 1227.8 cm^{-1}. The absolute intensity of the quarto C–H out of plane bend mode at 767.9 cm^{-1} increases slightly upon ionization. For the experimental [26] band at 1525.7 cm^{-1}, no theoretical band is reported. Theory predicts a strong band at 1498.8 cm^{-1} for which no experimental band is present.

The intense features present in the spectra of Anthracene cation are at 1213.3, 1325.4 and 1519.4 cm^{-1}. Barring a few modes, the theoretical spectra correlates well with the experimental spectra [28]. The intense experimental band at 1418.4 and at 1352.6 cm^{-1} have no theoretical counterparts.

The prominent modes in the spectra of Tetracene cation are at 1210.9, 1333.3, 1486.9 and 1511.9 cm^{-1}. While the band at 1511.9 cm^{-1} has no corresponding experimental [28] feature, the experimental band at 1543.3 cm^{-1} is far more intense (by more than an order of magnitude) than the theoretical band at 1533.1 cm^{-1}. Similar discrepancy exists for the experimental band at 1178.5 cm^{-1} for which the computed band at 1190.4 cm^{-1} is very weak in intensity.

The computed spectra of Pentacene cation has the most intense band corresponding to C–C stretch mode at 1343.8 cm^{-1} (1359.2 cm^{-1} in Langhoff's calculations [35]) and is assigned to an experimental [28] peak of moderate intensity at 1361.7 cm^{-1}. The experimental maximum intensity band at 1395.5 cm^{-1} is away from the theoretical maximum intensity mode. The intense experimental band at 1174.7 cm^{-1} is an order of magnitude greater in intensity than the computed one at

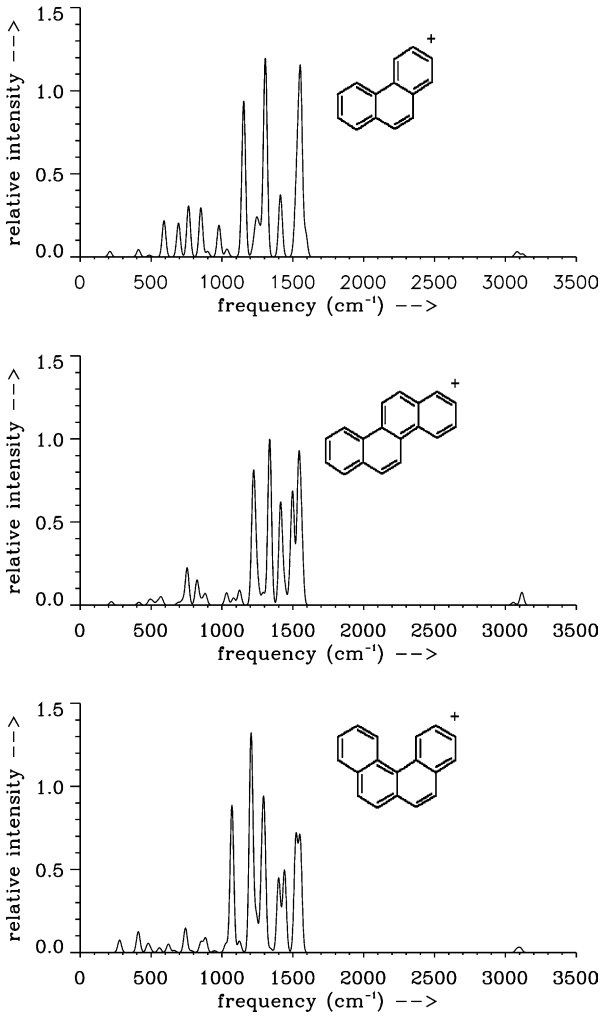

Fig. 6. Computed spectra of non-linear PAH cations.

1184.5 cm^{-1} and the calculated band at 1496.2 cm^{-1} is an order of magnitude more intense than the experimental feature at 1495.5 cm^{-1}.

Like other linear PAHs Hexacene and Heptacene cation spectra has intense features in the 1100–1500 cm^{-1} range. For Hexacene cation, the most intense feature is near 1350 cm^{-1} and the feature at 1490.2 cm^{-1} is nearly equal to it in intensity. In computed spectra of Heptacene cation the peak at 1483.2 cm^{-1} is the most intense band with the 1226.5 cm^{-1} feature nearly equal in intensity. The band at 1350.5 cm^{-1} corresponding to the 7.7 μm AIB is not as intense as in case of other polyacene cations. The spectra of larger polyacenes are simpler in comparison to the spectra of smaller molecules.

The computed spectra of non-linear PAHs is given in Fig. 6. The spectra of Phenanthrene cation shows a number of moderate and high intensity bands. The most intense feature predicted by our calculations is at 1555.1 cm^{-1} corresponding to the most intense experimental [27] band at 1565.0 cm^{-1}. The intensities of the C–H out of plane bend vibrations are much lower in the experimental data as compared to the theoretical ones. The intense feature at 1153.9 cm^{-1} has no corresponding experimental band while the peak at 1534.5 cm^{-1} does not match the relative intensity of the experimental counterpart.

In the spectra of Chrysene cation, no experimental [29] feature is obtained for the quarto Hydrogen wag feature at 754.3 cm^{-1}. The experimental feature at 1137.2 cm^{-1} is of high intensity while the corresponding theoretical band at 1124.1 cm^{-1} is nearly an order of magnitude less intense. The calculated most intense feature at 1336.9 cm^{-1} corresponds to an experimental band of high intensity at 1335.9 cm^{-1}, but the most intense experimental feature is at 1315.7 cm^{-1}, which is unassigned.

The comparison of the frequency and relative intensity for 3,4-Benzophenanthrene cation with that of Langhoff's [35] result is given in Table 3(b). The spectra of this PAH is very complex and consists of several intense bands in the range 1000–1600 cm^{-1}. Match with Langhoff's data is good but a few variations in intensity correlation are present. While Langhoff's data consists of several high intensity features nearly equal in intensity to the most intense band, this work predicts more features with moderate intensity. To the best of our knowledge, no experimental spectra is available to get a better overview of this cation.

The above comparisons of frequency and relative intensity of various neutral and ionized PAHs show that theoretical and experimental results disagree over very few band positions and relative intensities. In case of neutrals the intensity mismatch wherever present has the theoretical intensity on the higher side. Compared to neutrals, more discrepancies in frequency matching and intensity correlation with experimental data are present in cations. These discrepancies may be due to the experimental constraints in obtaining spectra of pure PAH cations and also due to the restrictions in carrying out the theoretical calculations. While the experimental results are affected by matrix involvements, contaminations, presence of neutral molecules in the spectra of cations and the presence of overtones and combination bands, the theoretical results are marred by the choice of basis sets and other computational restrictions.

3. Discussion

The Astrophysical infrared emissions depend on the excitation and internal conversion mechanisms in possible PAHs and result from transitions in higher vibrational levels. This may cause the emission features to be broader and slightly red shifted with respect to laboratory absorption bands. But no drastic changes between emission and absorption bands are observed in the few laboratory emission studies available [33,34],

wherein a good agreement with theoretical calculations is also shown. Therefore, comparison of interstellar IR spectra with laboratory absorption studies [16–29] and theoretical calculations [35–40] does strengthen the PAH–AIB hypothesis. The PAH hypothesis is also supported by studies related to photo-physical stability of PAHs in harsh environments of ISM [47–50].

The modelling of a composite spectra using combination of several PAHs to fit the observed Interstellar spectra, has shown that different PAH populations exist in different Astrophysical environments [46]. More cations are present in harsh environments of star forming regions while a mixture of neutrals and cations is in benign environments of Proto planetary-nebula. The PAH size distribution and charge state structure characterization shall lead to a better understanding of the origin of Interstellar spectra and thus, of the physical environments present therein.

The gross change in the spectra of cations, i.e., shift in band positions and intensity changes, warrants a closer look at the structural variations and changes in charge distribution on ionization of PAHs. The structural changes comprises mainly the changes in bond lengths of outer bonds in linear polyacenes. These bond length changes affect the vibrational force constant that is reflected in the spectra as band position shifts. A shorter bond implies shift towards higher wavenumber. Since, band positions vary little on ionization, it seems that small geometry changes do not affect much the overall vibrational force field of the PAHs.

It is the change in charge distribution upon ionization that affects dipole variations causing drastic intensity changes and in turn affecting the C–H stretch mode at 3.3 μm (3030 cm^{-1}) and the C–C stretch and C–H in plane bend modes between 6 and 9 μm (1100–1650 cm^{-1}). In case of linear polyacenes, maximum effect of ionization is on the outer Carbon atoms, therefore, these must be responsible for the increase in intensity of C–C stretch and C–H in plane bend modes in the spectra of cations. This is borne out by the fact that the high intensity modes in cations have maximum vibrational contributions from these outer carbons. In the non-linear PAHs, the charge variations depend on the shape of the catacondensate and no systematic charge variations could be identified.

In cations the C–H stretch intensity is reduced drastically but it gradually increases with the size of PAH and bears a more neutral like absolute intensity in very large species [51,52]. As the cation size increases the additional charge is distributed over larger number of atoms so large cations have lesser charge variation from neutrals. This suppression of C–H stretch intensity in cations of both linear and non-linear PAHs can be understood in terms of the charge on the H atoms. The C–H stretch intensity increases when the H atoms are less positive, as is the case in anions [53]. Our calculations on Naphthalene show that charge on H atoms is least positive (0.04) in anion, becomes more positive in neutral (0.13) and cation (0.21). The variation in absolute intensity of C–H stretch mode follows a reverse trend viz. 9.57, 3.14 and 0.03 $debye^2/amu\text{-}Å^2$ in Naphthalene anion, neutral and cation respectively. A similar trend is seen in other PAHs [53].

Though there seems to be a clear relation between C–H stretch intensity and charge on H atoms, the C–C stretch and C–H in plane bend modes show no such relation. These modes increase in intensity even in anions [35,53] showing that any variation from the neutral charge distribution causes large dipole variations for these modes. Studies on substituted PAHs [54–56] do show characteristics that may explain the intensity enhancements of C–C stretch and C–H bend modes. In particular it has been reported that addition of NH_2 group leads to increase in intensity of modes between 1300 and 1600 cm^{-1} [54,55]. The NH_2 group withdraws charge from the ring resulting in a pseudo-ionization and cation like enhancement of these modes. As the charge on H atoms remain unaltered the C–H stretch intensity shows no variation from neutral unsubstituted molecule.

Such substitutions or Nitrogen Hetrocycles [56] give the molecules a permanent dipole which is not present in the symmetric PAHs. Some of the symmetric vibrations which are inactive in PAHs will be active and may produce large intensities in substituted PAHs. A mode by mode comparison is essential for better understanding of charge effects, which is only possible when substitutions leave the molecular symmetry intact.

The effect of ionization on the intensity of C–H out of plane bend modes is insignificant. Charge on the H atoms affects the out of plane modes only in terms of frequency shifts. As the size of polyacene cation is increasing, number of solo Hydrogen atoms is increasing and so is the absolute intensity of the 900 cm^{-1} wag mode. Very small change is there in intensity of the 750 cm^{-1} wag of quarto Hydrogen atoms.

The main points reflecting the systematic changes in intensities and band positions with size and ionization of PAHs are:

- The position of the 900 cm^{-1} solo Hydrogen wag shifts to a bluer wavelength with increasing size of linear PAHs. The intensity of this mode also increases with size. When ionized, the band position of this mode for each polyacene shifts blue-wards and the intensity of the mode slightly decreases (Fig. 7).
- With increasing size, i.e., from Naphthalene to Heptacene, the frequency of the 750 cm^{-1} quarto Hydrogen wag mode lies at a higher and lower wavenumber alternately for even and odd number of rings (Fig. 7). The red shifting in polyacenes with odd number rings is due to a mixing of contribution from solo Hydro-

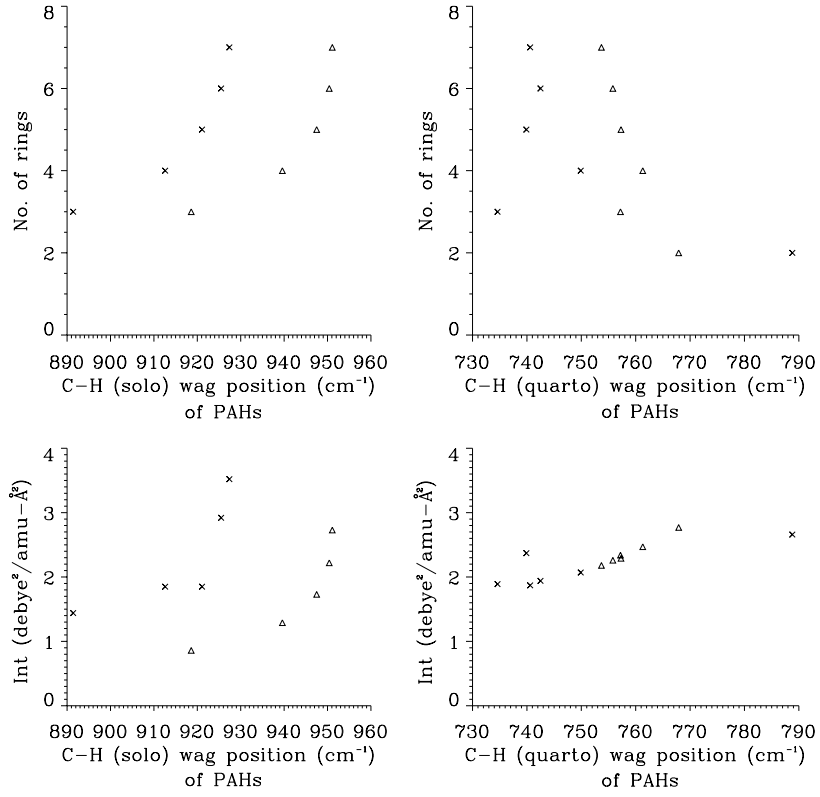

Fig. 7. Variation of band positions and intensity with size. Upper left: Shift in C–H solo wag position with size. Lower left: Intensity variations with size corresponding to the above figure. Upper right: Shift in C–H quarto wag position with size. Lower right: Intensity variations with size corresponding to the above figure. (×) denotes neutral PAHs, (△) denotes PAH cations (see text for detail).

gens. The solo–quarto mixing is much less in the even numbered counterpart. Naphthalene having no solo Hydrogen atom is highly blue shifted. The variation in the solo–quarto mixing is decreasing with increasing size leading to lesser wavenumber separation between even and odd number of rings. Intensity of this mode shows gradual increase with size. Similar effect of the solo–quarto mixing is present in cations. This mode shifts blue-wards and intensity increases upon ionization.

- In cations, the broad intense feature corresponding to the 7.7 μm AIB (1310 cm^{-1}) keeps on shifting blue-wards with increasing size. For Anthracene cation this band is at 1325.4 cm^{-1}, while for Heptacene cation it has shifted to 1350.5 cm^{-1}.

Table 4
Variation of position of bands with the number of rings in linear PAH cations

Polyacene	1200 (cm^{-1}) band[a]	1300 (cm^{-1}) band[a]	1500 (cm^{-1}) band[a]
Naphthalene	1228 (1.00)		1499 (0.48)
Anthracene	1213 (0.39)	1325 (1.00)	1519 (0.21)
Tetracene	1211 (0.23)	1333 (1.00)	1512 (0.30)
Pentacene	1254 (0.45)	1344 (1.00)	1496 (0.70)
Hexacene	1237 (0.77)	1355 (1.00)	1490 (0.98)
Heptacene	1227 (0.94)	1350 (0.83)	1483 (1.00)

[a] Relative intensities are given in parentheses.

- The 1610 cm^{-1} feature assigned to 6.2 μm AIB is shifting red wards with the increasing size of the cations and the intensity is increasing.

In PAH cations, the spectra of smaller PAHs consists of several moderate and intense peaks. As the size increases the spectra becomes smoother with fewer number of high intensity features. Larger PAH cations (Fig. 5) have just three major peaks. These peaks lie near the 1200, 1300 and 1500 cm^{-1} wave-numbers. The variation of band positions of these features of the cations with the size of PAHs is shown in Table 4. These modes are mainly due to C–H in plane bend and C–C stretch vibrations. To understand better the exact nature of these modes, plots exhibiting Normal vibrations are shown in Figs. 8–10 for 1200, 1300 and 1500 cm^{-1} modes. Fig. 8 shows that in all PAHs, major contribution to the mode near 1200 cm^{-1} is from the in plane bending of Hydrogen atoms. The inner central Carbons show translatory motions while only the outer bonds are involved in vibrations. The intensity of this mode is increasing with the size of the PAHs.

Vibrations for the most intense mode near 1300 cm^{-1} is shown in Fig. 9. It is clear that the motion of Hydrogens is less and the mode arises mainly from the stretching of C–C bonds. The central C–C bonds involving inner Carbon atoms have no vibrational motion and

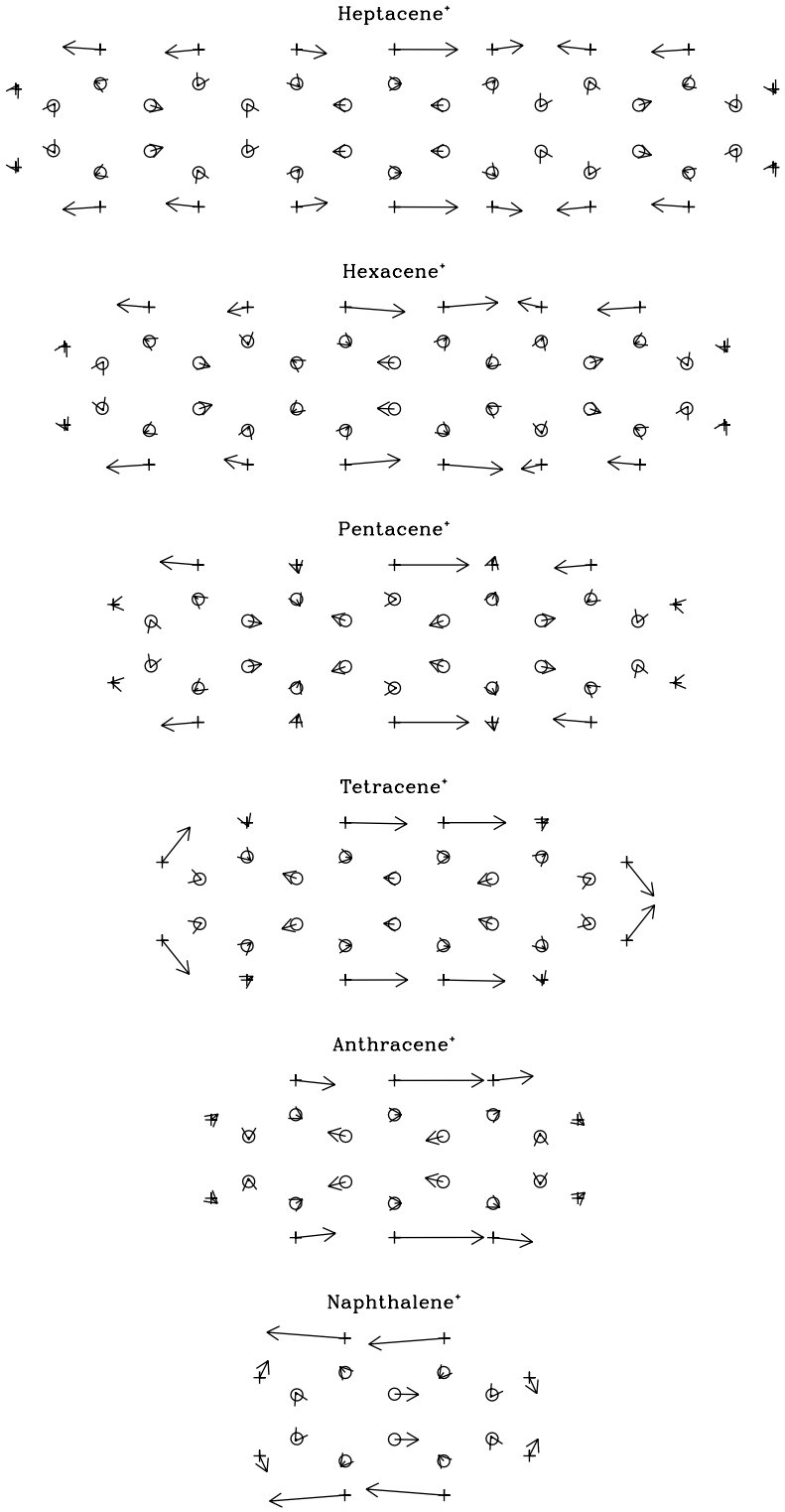

Fig. 8. The displacements of various atoms for 1200 cm^{-1} mode of Polyacene cations. (○) denote Carbons, (+) denote Hydrogens.

show translation in this mode as well. The involvement of outer bonds in this intense mode reaffirms that the change in charge distribution along outer bonds and atoms leads to increase in vibrational intensity. Fig. 10 gives the displacement of atoms for the peak near 1500 cm^{-1}. The vibrations in Heptacene, Hexacene and Pentacene are different from that of Tetracene, Anthracene and Naphthalene. Apart from C–C stretch, the central solo Hydrogens show large in plane vibrations in Pentacene, Hexacene and Heptacene and in

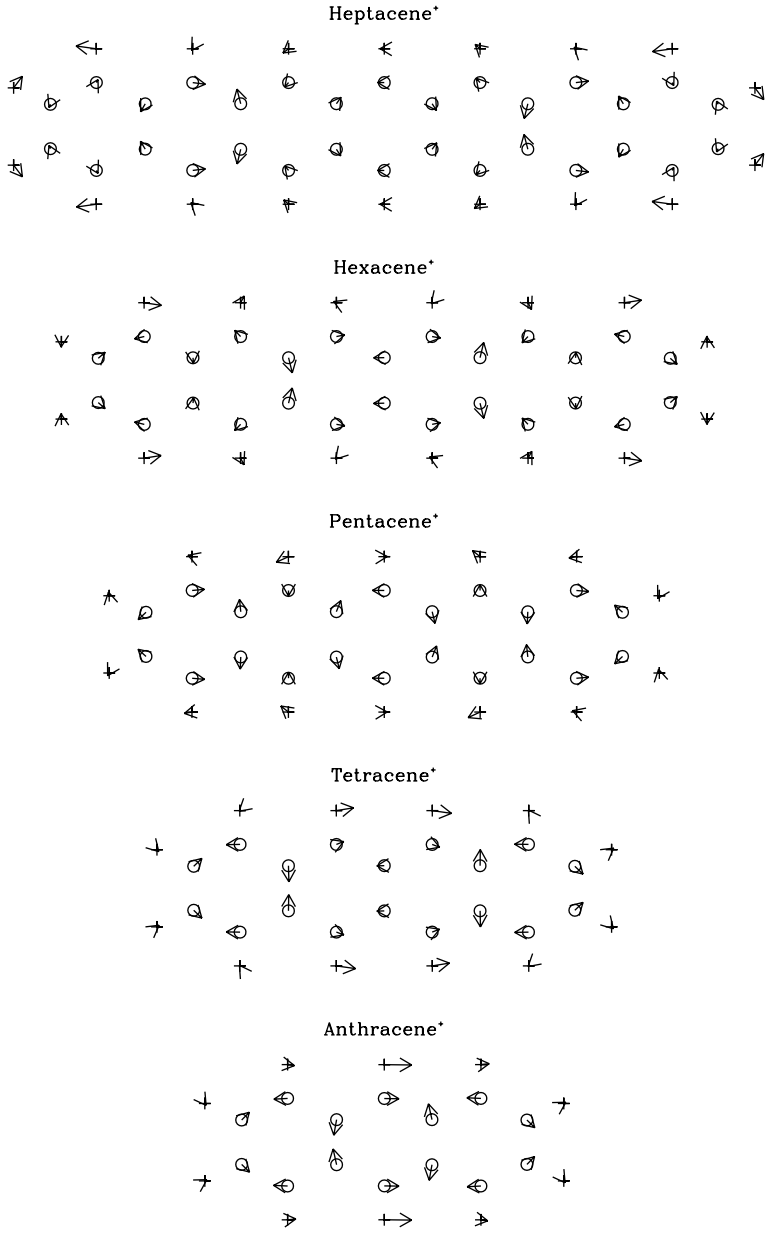

Fig. 9. The displacements of various atoms for 1300 cm^{-1} mode of polyacene cations. (○) denote carbons, (+) denote hydrogens.

smaller PAHs nearly all the Hydrogens including quarto Hydrogen atoms show in plane bending. As the PAH size increases this mode shows red shift and intensity increase due to coupling with lower frequency intense mode.

Since, the non-linear PAHs have different shapes, there is a non-systematic pattern in their spectra. The spectra of non-linear PAH cations has several features of high and moderate intensity unlike just three intense peaks in the spectra of linear PAH cations. The spectra of Chrysene and 3,4-Benzophenanthrene cations (Fig. 6) have several bands in the 1100–1600 cm^{-1} region while the spectra of Tetracene cation (Fig. 5), having same number of rings, is much simpler. The observed AIBs show a broad 7.7 μm band which correlates better with the spectra of non-linear PAH cations. On the other hand, corresponding to this band, a narrow peak is obtained in large polyacene cations.

The comparison between linear and non-linear PAHs having equal number of atoms shows that the geometry optimized energy is lower in non-linear PAHs. Anthracene has total energy $E = -538.487$ KJ/mole, while Phenanthrene has total energy $E = -538.496$ KJ/mole. Similarly total energies of Tetracene, Chrysene and 3,4-Benzophenanthrene are −691.826, −691.847 and −691.829 KJ/mole, respectively. There is little difference between total energies of linear and non-linear PAHs,

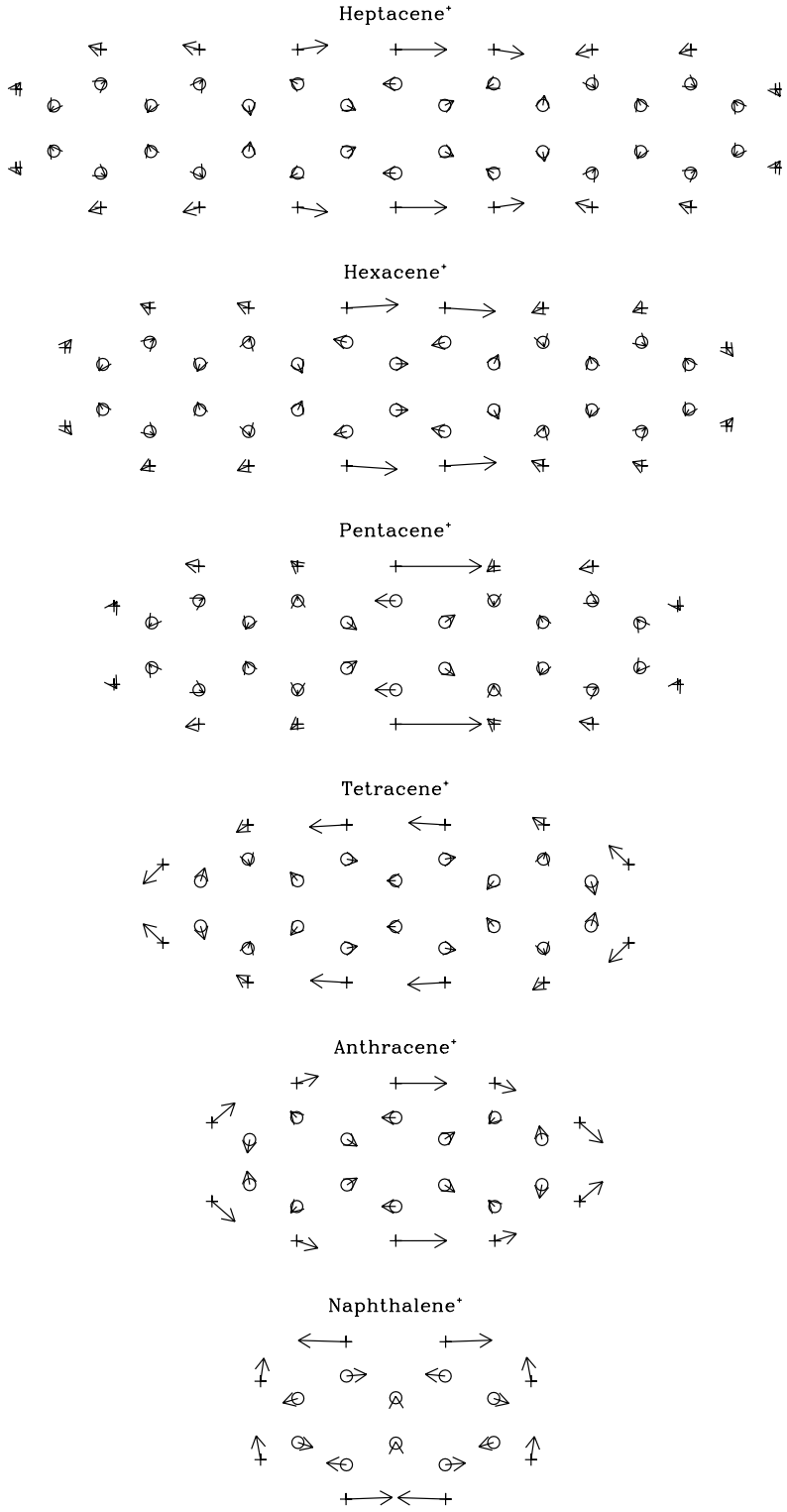

Fig. 10. The displacements of various atoms for 1500 cm^{-1} mode of polyacene cations. (○) denote carbons, (+) denote hydrogens.

still the lower energy of non-linear PAHs makes their formation in ISM slightly more probable. The steric hindrance between the bay region Hydrogen atoms of 3,4-Benzophenanthrene makes it less stable (higher energy) compared to Chrysene.

Observational studies are useful in estimation of PAH size and structure and their hydrogenated/dehydrogenated states in various Astrophysical environments [57–59]. The degree of hydrogenation/dehydrogenation has immense effect on the PAH spectra

especially on 10–15 μm range which depends on the type of Hydrogen atoms (solo, duo, trio or quarto) [60] attached to the peripheral Carbon atoms. The observed 6.2/7.7 μm ratio (0.39) [57] is in agreement for smaller PAH cations (Naphthalene (0.48), Anthracene (0.20) and Tetracene (0.29)). The 8.6/7.7 μm ratio (0.24) [57] matches that of Anthracene (0.39) and Tetracene (0.23) cations. The poor ratio matching shown by the larger catacondensed PAH cations makes them improbable to be the carriers of the AIBs as also their formation is less likely compared to non-linear PAHs. The study of more non-linear and compact PAH cations (pericondensed PAHs) is needed to get a better correlation and understanding of the carriers of AIBs.

4. Conclusions

The effect of ionization, as well as size and structure dependence, on spectra of catacondensed PAHs has been studied. The changes in intensities and band positions of various modes of PAH cations is consistent with experimental and other theoretical works. While the 11.2 μm and the 3.3 μm bands are intense ones in the spectra of neutral PAHs, the intensity of 6.2 and 7.7 μm peaks dominate in cations. The reason for these changes is the variation in the charge distributions and structure of the PAH molecules upon ionization. The C–H stretch mode intensity is related to the partial charge on the H atoms. For anions where the H atoms are less positive the intensity is large and it reduces in neutrals becoming negligible in cations as H atom charge becomes more positive. The C–C stretch and C–H in plane bend modes increase in intensity upon ionization. For linear PAHs the charge changes in outer Carbons result in this intensity increase.

Comparison with AIBs favour PAH cations over neutrals in most Astrophysical environments. The spectra of small polyacene and non-linear PAH cations present a better correlation with AIBs. Large polyacenes seem less probable to be the carrier of AIBs. The 7.7 μm AIB is a broad feature in the Astronomical spectra and corresponding feature of large polyacenes is a sharp peak whose match is poor. Moreover, the feature due to solo Hydrogens out of plane bend vibrations corresponding to the 11.2 μm AIB shifts blue-wards upon ionization. This blue shift increases with the size of PAH cations and Heptacene has this band at 10.5 μm. The smaller PAHs show a better matching in this context. Analysis of the region from 10 to 14 μm in the AIBs, which is due to the out of plane wag of Hydrogen atoms attached to the periphery of the rings, reveals that the AIB carriers must have significant number of solo Hydrogen atoms contributing to the 11.2 μm band. The weak bands beyond 11.5 μm point to possibility of duo, trio and quarto Hydrogens [59]. A detailed analysis of this region of the AIBs and its correlation with spectra of probable PAHs may give important information regarding the peripheral structure of contributing PAHs.

The variations in the AIBs from source to source and the interconnection of factors like the variation of spectra with ionization, degree of hydrogenation/dehydrogenation and size complicates identification of individual PAH in ISM. Nevertheless constraints on possible PAH states can be obtained by the study of band position shifts with PAH size and charge states. Compact PAHs have been favoured over catacondensed molecules because of their stability and also because of better spectral matching with AIBs. Study of the effect of ionization on pericondensed PAHs may reveal useful information about the ISM. A similar study for the pericondensed [in preparation] is being done to have a better understanding of these aspects.

Acknowledgements

The authors are thankful to Inter University Centre for Astronomy and Astrophysics, Pune for the use of computational and library facilities at the institute. This work was supported by Grants from Council of Science and Technology, Lucknow. A.P. acknowledges receipt of fellowships from CST, Lucknow and University Grants Commission, New Delhi. Fruitful comments and suggestions of the referees is acknowledged.

References

[1] M. Cohen, A.G.G.M. Tielens, J.D. Bregman, F.C. Witteborn, D.M. Rank, L.J. Allamandola, D. Wooden, M. de Muizon, Astrophys. J. 341 (1989) 246.
[2] T.R. Geballe, A.G.G.M. Tielens, L.J. Allamandola, A. Moorhouse, P.W.J.L. Brand, Astrophys. J. 341 (1989) 278.
[3] J.D. Bregman, L.J. Allamandola, A.G.G.M. Tielens, T.R. Geballe, F.C. Witteborn, Astrophys. J. 344 (1989) 791.
[4] M. Jourdain de Muizon, L. d'Hendecourt, T.R. Geballe, Astron. Astrophys. 227 (1990) 526.
[5] First ISO Results, Astron. Astrophys. 315 (1996) L26–L400.
[6] G.C. Sloan, T.L. Hayward, L.J. Allamandola, J.D. Bregman, B. DeVito, D.M. Hudgins, Astrophys. J. 513 (1999) L65.
[7] A. Leger, J.L. Puget, Astron. Astrophys. 137 (1984) L5.
[8] L.J. Allamandola, A.G.G.M. Tielens, J.R. Barker, Astrophys. J. 290 (1985) L25.
[9] J.L. Puget, A. Leger, Ann. Rev. Astron. Astrophys. 27 (1989) 161.
[10] L.J. Allamandola, A.G.G.M. Tielens, J.R. Barker, Astrophys. J. Supp. Ser. 71 (1989) 733.
[11] G.C. Clayton, K.D. Gordon, F. Salama, L.J. Allamandola, P.G. Martin, T.P. Snow, D.C.B. Whittet, A.N. Witt, M.J. Wolff, Astrophys. J. 592 (2003) 947.
[12] G.P. van der Zwet, L.J. Allamandola, Astron. Astrophys. 146 (1985) 76.
[13] A.G.G.M. Tielens, T.P. Snow, The Diffuse Interstellar Bands, Kluwer, Dordrecht, 1995.

[14] F. Salama, E. Bakes, L.J. Allamandola, A.G.G.M. Tielens, Astrophys. J. 458 (1996) 621.
[15] L. Biennier, F. Salama, L.J. Allamandola, J.J. Scherer, J. Chem. Phys. 118 (2003) 7863.
[16] J. Szczepanski, D. Roser, W. Personette, M. Eyring, R. Pellow, M. Vala, J. Phys. Chem. 96 (1992) 7876.
[17] J. Szczepanski, M. Vala, Nature 363 (1993) 699.
[18] J. Szczepanski, M. Vala, D. Talbi, O. Parisel, Y. Ellinger, J. Chem. Phys. 98 (1993) 4494.
[19] J. Szczepanski, C. Chapo, M. Vala, Chem. Phys. Lett. 205 (1993) 434.
[20] J. Szczepanski, M. Vala, Astrophys. J. 414 (1993) 179.
[21] M. Vala, J. Szczepanski, F. Pauzat, O. Parisel, D. Talbi, Y. Ellinger, J. Phys. Chem. 98 (1994) 9187.
[22] J. Szczepanski, C. Wehlburg, M. Vala, Chem. Phys. Lett. 232 (1995) 221.
[23] J. Szczepanski, J. Drawdy, C. Wehlburg, M. Vala, Chem. Phys. Lett. 245 (1995) 539.
[24] D.M. Hudgins, S.A. Sandford, J. Phys. Chem. A 102 (1998) 329.
[25] D.M. Hudgins, S.A. Sandford, J. Phys. Chem. A 102 (1998) 344.
[26] D.M. Hudgins, S.A. Sandford, L.J. Allamandola, J. Phys. Chem. 98 (1994) 4243.
[27] D.M. Hudgins, L.J. Allamandola, J. Phys. Chem. 99 (1995) 8978.
[28] D.M. Hudgins, L.J. Allamandola, J. Phys. Chem. 99 (1995) 3033.
[29] D.M. Hudgins, L.J. Allamandola, J. Phys. Chem. A 101 (1997) 3472.
[30] C. Joblin, L. d'Hendecourt, A. Leger, D. Defourneau, Astron. Astrophys. 281 (1994) 923.
[31] C. Joblin, P. Boissel, A. Leger, L. d'Hendecourt, D. Defourneau, Astron. Astrophys. 299 (1995) 835.
[32] D.J. Cook, R.J. Saykally, Astrophys. J. 493 (1998) 793.
[33] H.S. Kim, D.R. Wagner, R.J. Saykally, Phys. Rev. Lett. 86 (2001) 5691.
[34] H.S. Kim, R.J. Saykally, Astrophys. J. Supp. Ser. 143 (2002) 455.
[35] S.R. Langhoff, J. Phys. Chem. 100 (1996) 2819.
[36] F. Pauzat, D. Talbi, M.D. Miller, D.J. Defrees, Y. Ellinger, J. Phys. Chem. 96 (1992) 78.
[37] D.J. De Frees, M.D. Miller, D. Talbi, F. Pauzat, Y. Ellinger, Astrophys. J. 408 (1993) 530.
[38] F. Pauzat, D. Talbi, M.D. Miller, Y. Ellinger, Astron. Astrophys. 293 (1995) 263.
[39] F. Pauzat, D. Talbi, M.D. Miller, Y. Ellinger, Astron. Astrophys. 319 (1997) 318.
[40] F. Pauzat, Y. Ellinger, Chem. Phys. 280 (2002) 267.
[41] GAMESS M.W. Schmidt, K.K. Baldridge, J.A. Boatz, S.T. Elbert, M.S. Gordon, J.H. Jensen, S. Koseki, N. Matsunaga, K.A. Nguyen, S.J. Su, T.L. Windus, M. Dupuis, J.A. Montgomery, J. Comput. Chem. 14 (1993) 1347.
[42] F. Jensen, Computational Chemistry, John Wiley and Sons, New York, 2001.
[43] C.W. Bauschlicher, S.R. Langhoff, Spectrochim. Acta A 53 (1997) 1225.
[44] H. Yoshida, A. Ehara, H. Matsuura, Chem. Phys. Lett. 325 (2000) 477.
[45] H. Yoshida, K. Takeda, J. Okamura, A. Ehara, H. Matsuura, J. Phys. Chem. A 106 (2002) 3580.
[46] L.J. Allamandola, D.M. Hudgins, S.A. Sandford, Astrophys. J. 511 (1999) L115.
[47] W.A. Schutte, A.G.G.M. Tielens, L.J. Allamandola, Astrophys. J. 415 (1993) 397.
[48] T. Allain, S. Leach, E. Sedlmayr, Astron. Astrophys. 305 (1996) 616.
[49] C. Pech, C. Joblin, P. Boissel, Astron. Astrophys. 388 (2002) 639.
[50] V. Le Page, T.P. Snow, V.M. Bierbaum, Astrophys. J. 584 (2003) 316.
[51] D.M. Hudgins, C.W. Bauschlicher Jr., L.J. Allamandola, Spectrochim. Acta A 57 (2001) 907.
[52] C.W. Bauschlicher Jr., Astrophys. J. 564 (2002) 782.
[53] C.W. Bauschlicher Jr., E.L.O. Bakes, Chem. Phys. 262 (2000) 285.
[54] S.R. Langhoff, C.W. Bauschlicher, D.M. Hudgins, S.A. Sandford, L.J. Allamandola, J. Phys. Chem. A 102 (1998) 1632.
[55] C.W. Bauschlicher, Chem. Phys. 234 (1998) 87.
[56] A.L. Mattioda, D.M. Hudgins, C.W. Bauschlicher, M. Rosi, L.J. Allamandola, J. Phys. Chem. A 107 (2003) 1486.
[57] K.W. Chan, T.L. Roellig, T. Onaka, M. Mizutani, K. Okumura, I. Yamamura, T. Tanabe, H. Shibai, T. Nakagawa, H. Okuda, Astrophys. J. 546 (2001) 273.
[58] R. Vermeij, E. Peeters, A.G.G.M. Tielens, J.M. van der Hulst, Astron. Astrophys. 382 (2002) 1042.
[59] S. Hony, C. van Kerckhoven, E. Peeters, A.G.G.M. Tielens, D.M. Hudgins, L.J. Allamandola, Astron. Astrophys. 370 (2001) 1030.
[60] D.M. Hudgins, L.J. Allamandola, Astrophys. J. 516 (1999) L41.